Slow crossover in YbXCu$_4$ (X=Ag, Cd, In, Mg, Tl, Zn) intermediate-valence compounds

J. M. Lawrence
University of California, Irvine, California 92697

P. S. Riseborough
Temple University, Philadelphia, Pennsylvania 19122

C. H. Booth
Lawrence Berkeley National Laboratory, Berkeley, California 94720

J. L. Sarrao and J. D. Thompson
Los Alamos National Laboratory, Los Alamos, New Mexico 87545

R. Osborn
Argonne National Laboratory, Argonne, Illinois 60439
(Received 6 June 2000; published 11 January 2001)

We compare the results of measurements of the magnetic susceptibility $\chi(T)$, the linear coefficient of specific heat $\gamma(T)=C(T)/T$, and $4f$ occupation number $n_f(T)$ for the intermediate-valence compounds YbXCu$_4$ (X=Ag, Cd, In, Mg, Tl, Zn) to the predictions of the Anderson impurity model, calculated in the noncrossing approximation (NCA). The crossover from the low temperature Fermi-liquid state to the high-temperature local-moment state is substantially slower in the compounds than predicted by the NCA; this corresponds to the ''protracted screening'' recently predicted for the Anderson lattice. We present results for the dynamic susceptibility, measured through neutron-scattering experiments, to show that the deviations between theory and experiment are not due to crystal-field effects, and we present x-ray-absorption fine-structure results that show the local crystal structure around the X atoms is well ordered, so that the deviations probably do not arise from Kondo disorder. The deviations may correlate with the background conduction electron density, as predicted for protracted screening.

DOI: 10.1103/PhysRevB.63.054427 PACS number(s): 75.30.Mb, 75.20.Hr, 71.27.+a, 71.28.+d

I. INTRODUCTION

The rare-earth intermediate valence (IV) compounds[1] are moderately heavy fermion compounds where the characteristic (Kondo) energy is large compared to the crystal-field splitting ($T_K > T_{cf}$). Unlike the truly heavy fermion (HF) compounds[2] (where $T_K < T_{cf}$) the IV compounds do not reside close to a quantum critical point for a transition to antiferromagnetism, so non-Fermi-liquid behavior is neither expected nor observed and the scaling behavior that is observed does not reflect proximity to such a phase transition.[3] Furthermore, most of the IV compounds are cubic, so that anisotropy and low dimensionality are not issues. Hence the IV compounds are physical realizations of the isotropic orbitally degenerate ($N_J=2J+1=8$ for Yb) Anderson lattice model[4] for three spatial dimensions. This is an archetypal problem that is both simple and elegant for exploring the physics of electronic correlations in solids.

A key issue for the Anderson lattice is the role of lattice coherence, which can be thought of as dispersive or bandlike behavior of the $4f$ electrons or alternatively as correlations between the $4f$ electrons on different lattice sites. This contrasts the Anderson lattice (AL) with the Anderson impurity model (AIM) where no such coherence is present. For the HF and IV compounds the transport behavior, which depends crucially on the periodicity of the scattering potential, clearly manifests lattice coherence: the low-temperature resistivity (which is finite for the AIM) vanishes for the periodic compounds, as expected for a system obeying Bloch's law;[1,2] the de Haas–van Alphen signals are characteristic of renormalized f bands,[5] and the optical conductivity exhibits a Drude response at low temperatures that also reflects renormalized masses. [6] On the other hand, the dynamic susceptibility $\chi''(\omega)$ shows a Lorentzian power spectrum with very little Q dependence,[7] suggesting that the spin/valence fluctuations are very local and uncorrelated, as expected for the AIM, and thermodynamic properties that are dominated by the spin/valence fluctuations such as the temperature dependence of the susceptibility $\chi(T)$, specific heat $C(T)$ and $4f$ hole occupation number $n_f(T)$ (the Yb valence is $z=2+n_f$) seem to follow the predictions of the AIM, at least qualitatively.[8,9] Recent theory[10] of the Anderson lattice suggests, however, that there should be observable differences between the behavior of the AL and the AIM for these quantities. In particular, ''protracted screening'' can occur in the AL, which means that the crossover from the low-temperature Fermi-liquid state to the high-temperature local-moment state is slower for the lattice case than for the impurity case.

Protracted screening has been invoked[11] to explain photoemission results[12] which show far less temperature dependence than expected based on the AIM. Such results are controversial.[13] To search for such effects in the bulk thermodynamic behavior we herein compare our measurements[14]

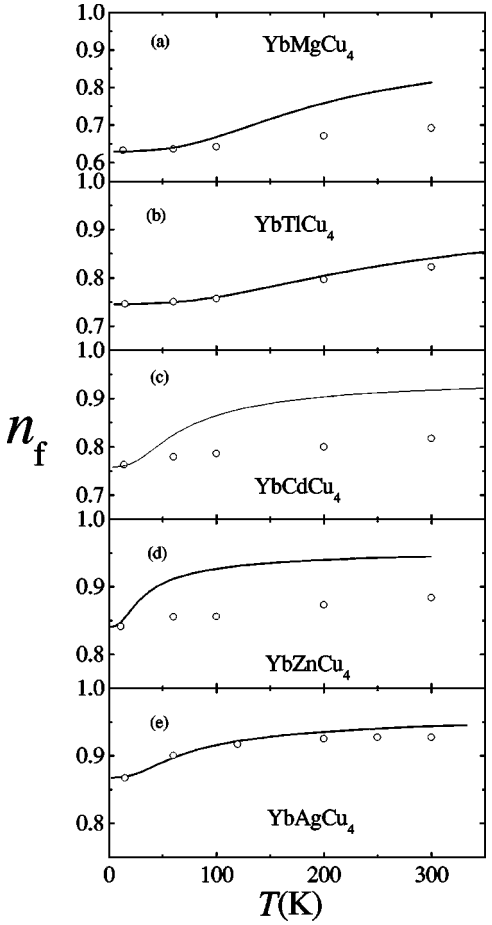

FIG. 1. The $4f$ hole occupation number $n_f(T)$ versus temperature for the YbXCu$_4$ compounds. The open circles are the experimental data and the solid lines are the predictions of the Anderson impurity model (AIM), with input parameters given in Table I.

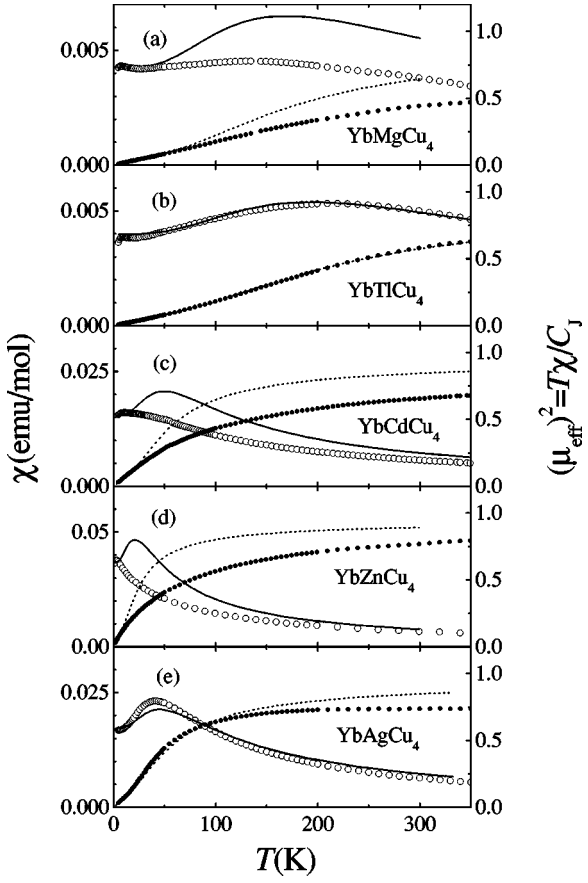

FIG. 2. The magnetic susceptibility $\chi(T)$ (open circles) and the effective moment $\mu_{eff}^2 = T\chi/C_J$ (solid circles) for the YbXCu$_4$ compounds. The solid (dotted) lines are the prediction of the AIM for the susceptibility (effective moment).

of $\chi(T)$, $C(T)$, and $n_f(T)$ for the series of related cubic ($C15b$) compounds YbXCu$_4$ (X=Ag, Cd, In, Mg, Tl, and Zn) to the predictions of the Anderson impurity model, calculated within a single approximation scheme, the noncrossing approximation (NCA). By making this comparison for several measurements for several related compounds, we put strong constraints on the applicability of the model. In addition, we include measurements of the dynamic susceptibility $\chi''(\omega)$ for X=Ag, Mg, Tl, and Zn; these allow us to determine whether the deviations from AIM behavior could arise from crystal-field effects and also give a fourth experiment for comparison to the predictions of the model. Finally, we include measurements of the x-ray-absorption fine-structure (XAFS) from the X-atom K edges for YbXCu$_4$ and X=Ag, Cd, and In and the L_3 edge for X=Tl to determine whether deviations from AIM behavior could arise from local lattice disorder in the samples.

II. EXPERIMENTAL DETAILS

The data for the $4f$ occupation number $n_f(T)$ (Fig. 1), the susceptibility $\chi(T)$ (Fig. 2), and the linear coefficient of specific heat $\gamma = C/T$ (Table I) are taken from Sarrao *et al.*[14] As explained in that paper, the samples were small, high quality single crystals grown in XCu flux. The specific heat was measured using a thermal relaxation technique. The susceptibility was measured using a superconducting quantum interference device magnetometer. In this work we have subtracted a small ''Curie tail'' (with Curie constant typically of order 10^{-2} emu K/mol) from the susceptibility. The occupation number $n_f(T)$ was determined from the near-edge structure in Yb L_3 x-ray-absorption measurements.

The neutron-scattering measurements were performed in the time-of-flight mode using the LRMECS spectrometer at IPNS (Argonne National Laboratory). The experimental conditions were similar to those discussed in a recent study[15] of YbInCu$_4$; we refer the reader to that publication for a more detailed account. The temperature of the measurement was 10 K, which is considerably smaller than T_K in each case. The samples utilized in these experiments were powders, typically of 50 g mass, grown from the melt inside evacuated tantalum tubes for X=Ag, Mg, and Zn; for X=In and Tl, a large number of single crystals grown as described in Sarrao *et al.*[14] were powdered to form the sample. The susceptibilities of these samples were identical to those shown in Fig. 2 except for X=Ag, where the temperature T_{max} of the maximum in the susceptibility was 10% smaller for the neutron sample, and for X=Tl where a fraction of the crystals used

TABLE I. Input parameters W, E_f, and V for the AIM calculation; the calculated Kondo temperature T_K; and the theoretical and experimental values of the specific-heat coefficient γ, the Wilson ratio $\mathcal{R}$, and the neutron line-shape parameters E_0 and Γ.

Compound	W (eV)	E_f (eV)	V (eV)	T_K (K)	γ (mJ/mol K^2)	$\mathcal{R}$	E_0 (meV)	Γ (meV)
YbTlCu$_4$	1.286	−0.50146	0.2195	514	32.1	1.26	54.0	31.2
				Expt:	24.2	1.67	38.8	32.3
YbMgCu$_4$	1.005	−0.1897	0.128	500	36.7	1.22	44.6	23.4
				Expt:	53.3	0.84	31.9	34.5
YbInCu$_4$	1[a]	−0.7442	0.232	299	41.3	1.44	41.6	25.9
				Expt:	41.3[a]	1.44[a]	41.6	13.5
YbCdCu$_4$	0.929	−0.17576	0.098	127	120.4	1.40		
				Expt:	165.6	1.02		
YbAgCu$_4$	0.865	−0.4485	0.148	95	137.9	1.29	11.3	7.1
				Expt:	198.9	0.89	9.8[b]	6.0[b]
YbZnCu$_4$	1.213	−0.1984	0.1038	60	296.8	1.33	5.0	4.1
				Expt:	370	1.07	7.4	6.1

[a]The values of W are deduced from the specific heat of the corresponding LuXCu$_4$ compound and the experimental specific-heat coefficients have been corrected for the non-4f contribution by subtracting the specific-heat coefficient of the LuXCu$_4$ compound. Since the ground state of LuInCu$_4$ is semimetallic (Ref. 19) and does not serve for these estimates, we have arbitrarily set W=1 eV and we have subtracted a corresponding amount (8.7 mJ/mol K^2) from the specific-heat coefficient.

[b]For comparison to theory these values should be increased by 10% to account for the fact that the neutron-scattering sample had a Kondo temperature that is 10% smaller than the sample used to measure χ and n_f.

to create the powder had large Curie tails indicative of disorder or impurities. For each sample, given that the elastic energy resolution full width at half maximum varies as $\delta E \sim 0.07$–$0.1E_i$, we used several incident neutron energies E_i (e.g., 35, 80, and 150 meV) to give greater dynamic range in energy transfer ΔE for the measurement. To improve statistics we took advantage of the lack of Q dependence of the magnetic scattering[7] and grouped detectors into three bins, with average scattering angle 20° (low Q), 60°, and 100° (high Q). The scattering was put on an absolute scale by comparison to the measured scattering of a vanadium sample. We also measured the scattering of YAgCu$_4$, LuMgCu$_4$, YMgCu$_4$, YTlCu$_4$, and LuZnCu$_4$ in order to help determine the nonmagnetic scattering.

The XAFS experiments were performed on Beam Line 4-3 at the Stanford Synchrotron Radiation Laboratory (SSRL) using a half-tuned Si(220) double-crystal monochromator. Samples were ground, passed through a 30-μm sieve and brushed onto transparent tape. Pieces of tape were stacked such that the change in the absorption at the Yb $L_{\rm III}$ edge was $\lesssim$ unity. The samples were the same flux-grown crystals as used in Sarrao *et al.*[14] and whose susceptibilities are shown in Fig. 2. For temperature control, we utilized a L He flow cryostat.

III. THEORETICAL DETAILS

The predictions of the Anderson impurity model were calculated in the noncrossing approximation (NCA).[16] This approximation allows for calculation of all relevant experimental quantities, both static (χ, n_f, $\gamma=C/T$) and dynamic [$\chi''(\Delta E)$], for realistic orbital degeneracy and for realistic spin-orbit and crystal-field splitting. It agrees well[16] over a broad temperature range with calculations using the Bethe ansatz, but does produce spurious and unphysical non-Fermi-liquid artifacts in the low-frequency density of states and in the dynamic susceptibility at very low temperatures.[17] These artifacts are not significant for the temperatures and frequencies studied here. The conduction band was assumed to have a Gaussian density of states of width W and centered at the Fermi energy, i.e., $N(\varepsilon)=e^{-\varepsilon^2/W^2}/(\sqrt{\pi}W)$. The hybridization matrix elements were assumed to be **k** independent, i.e., $V_{kf}=V$, which may be a good approximation if the thermodynamic and magnetic properties are predominately determined by the conduction-band states within kT_K of the Fermi energy. The finite temperature NCA self-consistency equations[16,18] were solved using three overlapping linear meshes. The thermodynamic and spectroscopic results for Ce impurities with spin-orbit splitting and in various crystal fields were compared with those published in Bickers *et al.*[16] and good agreement was found despite the difference in procedure and the different choice of conduction-band density of states.

For Yb IV compounds where crystal fields can be ignored the magnetic orbital degeneracy is $N_J=8$ and there are essentially four input parameters for the AIM calculation: the spin-orbit splitting (which we fixed at $\Delta_{so}=1.3$ eV, the value typically observed in photoemission experiments[12]), the width W of the Gaussian conduction band, the hybridization constant V, and the f-level energy (relative the Fermi level) E_f. Since it is only the conduction states within $\max\{kT,kT_K\}$ of the Fermi level that contribute significantly

to the experimental quantities discussed here, the bandwidth parameter W must be chosen to give the correct value of $N(\epsilon_F)$ for the background conduction band. Assuming the background band states in YbXCu$_4$ are similar to those in LuXCu$_4$, we choose W to reproduce the linear specific-heat coefficient γ (Lu) of the corresponding LuXCu$_4$ compounds,[14] using the free-electron approximation to convert the measured value of γ (Lu) to $N(\epsilon_F)$. This is an important constraint since (as we found in the earlier paper[14]) it is possible to force fits to $n_f(T)$ over the whole temperature range if unrealistically small values of the bandwidth are used in the model. In YbXCu$_4$ compounds, the valence bands have a width of order 10 eV;[19,20] since the 2σ full width of the Gaussian band is $\simeq 4W$, the values of W ($\simeq 1$ eV, see Table I) obtained from γ(Lu) are quite reasonable.

Once Δ_{so} and W are fixed, V and E_f can be uniquely determined by fitting to the ground-state values of the susceptibility and occupation number. The values of these parameters are given in Table I; the Kondo temperature is calculated from the formula

$$T_K = \left(\frac{V^2}{\sqrt{\pi}W|E_f|}\right)^{1/8}\left(\frac{W}{\Delta_{so}}\right)^{6/8} W e^{\sqrt{\pi}WE_f/8V^2} \quad (1)$$

which includes the effect of spin-orbit splitting but ignores crystal-field splitting.

For these values of input parameters, we calculated the frequency dependence of the dynamic susceptibility at 10 K and the temperature dependence of the static susceptibility, the $4f$ occupation number, and the free energy. From the latter we determined the linear coefficient of specific heat by fitting to the formula $F = E_0 - (\gamma/2)(T/T_K)^2$ in the temperature range $0.03 \leqslant (T/T_K) \leqslant 0.07$; the values of γ so determined have a systematic error of order 5–10%.

IV. RESULTS AND ANALYSIS

A. Neutron scattering

The primary goal of the neutron-scattering measurements was to determine whether crystal-field excitations can be resolved in these compounds. Determination of the magnetic scattering in polycrystals of IV compounds requires correct subtraction of the nonmagnetic scattering. We have adopted a variant on the conventional procedure[21] for accomplishing this where the YXCu$_4$ (and/or LuXCu$_4$) nonmagnetic counterpart to the corresponding YbXCu$_4$ sample is measured to determine the factor $h(\Delta E) = S(\text{high } Q;\Delta E;\text{Y})/S(\text{low } Q;\Delta E;\text{Y})$ by which the high-Q scattering (which is almost totally nonmagnetic scattering) scales to the low Q values where the magnetic scattering is strongest. This factor varies smoothly from a value ~ 4–5, at $\Delta E = 0$, to a value of 1 at large ΔE where Q-independent multiple scattering dominates the nonmagnetic scattering. [When this decrease in $h(\Delta E)$ is neglected the nonmagnetic scattering will be underestimated at large energy transfer.] In addition we have included an energy-independent multiplicative factor κ which is needed to account for the fact that the multiple scattering, which dominates the low-Q nonmagnetic scattering, has different strengths for Yb than for Y or Lu. (When this factor is neglected the magnetic scattering is overestimated.) That is, we determine the magnetic scattering from the formula

$$S_{mag}(\text{low } Q) = S_{tot}(\text{low } Q) - \kappa h(\Delta E) S_{tot}(\text{high } Q). \quad (2)$$

The magnetic scattering is related to the dynamic susceptibility through the formula

$$S_{mag} = \frac{2N}{\pi\mu_B^2} f^2(Q)(1 - e^{-\Delta E/k_B T})^{-1}\chi''(Q,\Delta E), \quad (3)$$

where $f^2(Q)$ is the Yb $4f$ form factor. For each κ we fit the dynamic susceptibility assuming that it is Q independent and assuming a Lorentzian power spectrum:

$$\chi''(Q,\Delta E) = \chi_{dc}(T)\Delta E\left(\frac{\Gamma}{2\pi}\right)\left[\left(\frac{1}{[(\Delta E - E_0)^2 + \Gamma^2]}\right) + \left(\frac{1}{[(\Delta E + E_0)^2 + \Gamma^2]}\right)\right]. \quad (4)$$

The prediction of the Anderson impurity model for χ'' at $T \ll T_K$ also can be fit to this formula; we have included in Table I the values of E_0 and Γ deduced from the fits to the NCA results. The fits to the experimental data include corrections for absorption and for instrumental resolution. The data for every E_i are included in the fit. We then find the value of κ that gives the smallest reduced χ^2 for the fit. The best-fit values of κ were consistently in the range 0.65–0.75; furthermore, the best-fit values of κ gave better agreement (10–20%) between the fit value of χ_{dc} and the value shown in Fig. 2 than was seen for $\kappa = 1$. Use of this multiplicative factor also leads to excellent agreement between the values of magnetic scattering estimated at different incident energies. In Fig. 3 we show the data (symbols) for the magnetic scattering at low Q (fixed average scattering angle $\phi = 20°$) and the fits (solid lines). (Plots of the data for YbInCu$_4$ are given in the earlier publication.[15]) We note that in the time-of-flight experiment Q varies with both E_i and ΔE at fixed ϕ and consequently the form factor, the absorption and the instrumental resolution all depend on E_i; this explains why the data and the fits for different E_i do not overlap. The parameters E_0 and Γ for the best fits are given in Table I, where they are compared to the values predicted by the AIM calculation. We note that our results agree well with an earlier measurement of YbAgCu$_4$.[22] Although the fits are of reasonable statistical quality with reduced $\chi^2 \simeq 1$, the degree of systematic uncertainty due to the assumptions made about the nonmagnetic scattering is unknown. The problem is especially serious for IV compounds where T_K is large so that large incident energies are required, with the result that multiple scattering is large. To be cautious, we expect a 10% error in the determination of E_0 and Γ.

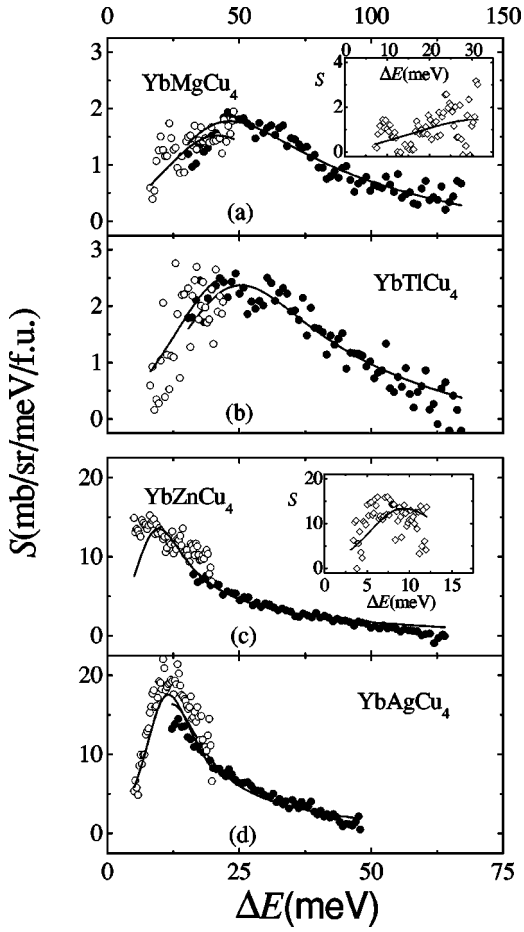

FIG. 3. The inelastic magnetic neutron-scattering spectra for the YbXCu$_4$ compounds at $T=10$ K. For each sample, two or three values of the incident energy E_i were used to increase the dynamic range. (YbMgCu$_4$: solid circles, $E_i=150$ meV; open circles, $E_i=80$ meV; open diamonds, $E_i=35$ meV. YbTlCu$_4$: solid circles, $E_i=150$ meV; open circles, $E_i=80$ meV. YbZnCu$_4$: solid circles, $E_i=80$ meV; open circles, $E_i=25$ meV; open diamonds, $E_i=15$ meV. YbAgCu$_4$: solid circles, $E_i=60$ meV; open circles, $E_i=25$ meV.) The solid lines represent fits to the Lorentzian power spectrum (see text) with the parameters given in Table I.

B. XAFS

The primary goal of the XAFS measurements was to determine whether X/Cu site interchange is significant in these compounds. Such disorder is a real possiblity given that YbCu$_5$ can grow in the $C15b$ structure,[23] and given that UPdCu$_4$, which also grows in the $C15b$ struucture, has been shown to have significant Pd/Cu site interchange.[24] Our earlier neutron-diffraction measurements[25] of flux-grown crystals of YbInCu$_4$, coupled with Rietveld refinement, suggest the average crystal structure is very well ordered. We employ the XAFS technique here both because the measurement does not depend on lattice periodicity (i.e., it is a local probe and is thus complimentary to diffraction) and because it is atomic-species specific. In such a measurement, a fine-structure function $\chi(k)$ is extracted from the absorption data and related to the radial bond-length distribution around the absorbing X atomic species. This measurement is particularly sensitive to X/Cu site interchange because if any X atoms rest on the Cu sites, a short X-Cu bond length at about 2.55 Å will appear that corresponds to the Cu-Cu nearest-neighbor bond length in the nominal structure. This bond length is significantly shorter than the nearest-neighbor X-Cu pairs at ~2.93 Å or the X-Yb pairs at ~3.06 Å, and so is easy to resolve if the site interchange is frequent. In addition to searching for X/Cu site interchange, we also look for more generic disorder in the nominal X-Cu and X-Yb pairs by analyzing the distribution widths extracted from the r space fits as a function of temperature between 15 and 300 K. Bond-length distribution widths should follow a correlated-Debye model[26] as a function of temperature if the structure does not have any static (positional) disorder. This model differs from the usual Debye model because it includes the correlations in the motions between the atoms in a given pair. It has been shown to be accurate to within ~5% for metals.[27] Any static disorder should manifest as a constant offset, as is clearly shown, for example, for La$_{1-x}$Ca$_x$MnO$_3$.[28]

The XAFS data were fit in r space, following procedures in Refs. 24 and 27. Initial fits included a short X-Cu pair at ~2.55 Å. The relative amplitude of this peak compared to the amplitude of the nominal X-Cu at ~2.93 Å gives the percentage of X atoms on Cu sites. Errors in this measurement were determined by assuming that the fitted statistical χ^2 was equal to the degrees of freedom in the fit as given by Stern[29] and then increasing the amount of site interchange until χ^2 increased by one, while allowing all the other parameters in the fit to vary. These results are presented in Table II. For X=In, Cd, and Ag the site interchange has the same value as the error, and hence the results are consistent with the zero site interchange. For YbTlCu$_4$ the error is smaller than the site interchange but it is also smaller than

TABLE II. XAFS fit results between 2.0 and 3.2 Å. Fits only include the nominal structural peaks X-Cu at ~2.9 Å and X-Yb at ~3.06 Å. S_0^2 is an amplitude reduction fact that sets the scale for the distribution variance measurements. See text for details.

		Θ_{cD} (K)		σ^2_{stat} (Å^2)		X/Cu
X	S_0^2	Cu	Yb	Cu	Yb	Interchange
Tl	0.89(5)	230(5)	230(5)	0.0005(4)	0.0005(5)	4(1)%
In	1.04(5)	252(5)	280(5)	0.0009(4)	0.0011(5)	2(3)%
Cd	0.98(5)	240(5)	255(5)	0.0007(4)	0.0010(5)	5(5)%
Ag	0.91(5)	250(5)	235(5)	0.0008(4)	0.0006(5)	2(2)%

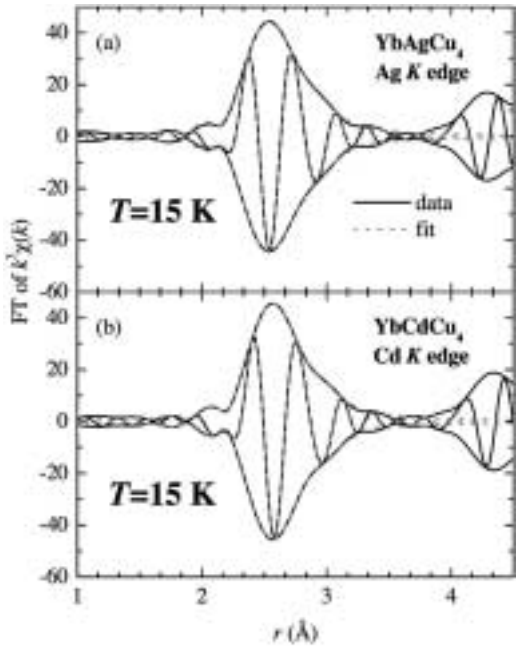

FIG. 4. XAFS data and fits on (a) $YbAgCu_4$ and (b) $YbCdCu_4$. The outer envelope shows $\pm$ the amplitude (or modulus) and the oscillating inner curve is the real part of the complex Fourier transform of $k^3\chi(k)$. The r axis includes different phase shifts for each coordination shell, so that the r of a given peak appears somewhat longer than the actual pair distance R. These transforms are from 2.5 to 15 Å^1 and Gaussian narrowed by 0.3 Å^{-1}. Fits are from 2.0 to 3.2 Å.

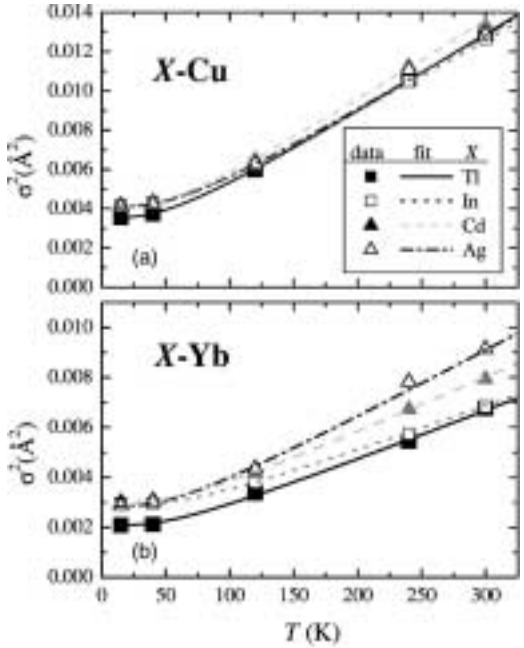

FIG. 5. The variance in (a) the X-Cu pair distribution at $\sim$2.9 Å, and (b) the X-Yb pair distribution at $\sim$3.06 Å. The temperature dependence follows a correlated-Debye model well for all the data, as shown. Most of the low-temperature data are very similar, except the Tl-Cu and Tl-Yb σ^2's are somwhat lower due to the greater mass of Tl compared to the other X's.

the error in the other cases. Furthermore, the fitted Tl-Cu bond length was very low (2.40 Å) even though Tl has the largest atomic radius of all the X's measured. We note that sytematic errors in the fit can arise from use of an incorrect theoretic backscattering amplitude.[27] Given all this, we think that the error is underestimated for $YbTlCu_4$. Therefore we conclude that, within $\sim$3%, none of the materials measured have any X/Cu site interchange.

Once the lack of site interchange was determined, we fit the data assuming no site interchange and determined the pair distribution widths to search for any other disorder. Examples of two of these fits are shown in Fig. 4. The bond lengths of the nominal X-Cu and X-Yb pairs do not deviate from the average $C15b$ structure assuming lattice parameters from Ref. 14 by more than 0.02 Å. The distribution widths are shown in Fig. 5, as are the fits to the correlated-Debye model. Parameters of the correlated-Debye fits are given in Table II. The fits are quite good and the observed values of the static disorder σ^2_{stat} are typical of values seen in well-ordered compounds.

C. Susceptibility, 4*f* occupation number, and specific heat

The results of our calculations for $\chi(T)$ and $n_f(T)$ for the different $YbXCu_4$ compounds are shown in Figs. 1 and 2 where they are compared to the experimental behavior.[14] The most noteable feature is that for $X=$Cd, Mg, and Zn, the experimentally determined occupation number $n_f(T)$ and the effective moment $\mu^2_{eff}=T\chi/C_J$ (where C_J is the $J=7/2$ Curie constant) rise towards the high-temperature limit more slowly than predicted by the impurity theory. The effect is somewhat weaker but still apparent for $X=$Ag. For $X=$Tl the experimental occupation number shows a weak retardation compared to theory but the experimental susceptibility tracks the impurity theory up to room temperature. The linear coefficients of specific heat determined from our calculation are given in Table I where they are compared to the experimental values; the experimental and calculated values of the Wilson ratio $\mathcal{R}=(\pi^2R/3C_J)\chi(0)/\gamma$ are also compared in the table.

V. DISCUSSION

Figures 1 and 2 give our basic result: the crossover from the ground-state Fermi liquid to the high-temperature local moment state is slower for the real materials than predicted by the Anderson impurity model.

There are several reasons why this comparison to theory might be incorrect. The first is that crystal fields may be large in these compounds. Crystal fields can cause the ground-state multiplet to have a lower degeneracy than the value $N_J=8$ expected for $J=7/2$. Since the AIM results depend on N_J this could lead to a discrepancy between theory and experiment if N_J were incorrectly assigned in the calculation. Indeed, in the earlier paper[14] we found that for some cases we could fit the data assuming a lower degeneracy, e.g., $J=5/2$ for $YbMgCu_4$. Our inelastic magnetic neutron-scattering experiments were designed to test for this possi-

bility. As mentioned above, there is a systematic error of order 10–20% in the determination of the peak position and width of the magnetic scattering. For our present purposes, however, the basic point is that the data can be well fit by a single broadened Lorentzian whose peak energy E_0 is in reasonable accord with the predicted value (i.e., it is of order T_K); there are no sharp crystal field levels in evidence. This also is in accord with the fact that the crystal fields seen in trivalent compounds such as YbInNi$_4$ (Ref. 30) or YbAuCu$_4$ (Ref. 22) are of order 2–4 meV which is significantly smaller than T_K for most of these compounds.

A second potential problem for our analysis is that if Yb atoms are in a disordered environment, there can be a distribution of Kondo temperatures. In this case, the measured susceptibility involves an integral over this distribution of Kondo temperatures, which would spread the crossover over a broader range of temperature.[24,31] This effect may be relevant in UPdCu$_4$, where there is significant ($\approx$25%) Pd/Cu site exchange.[24] Our XAFS results for the YbXCu$_4$ compounds show that within $\simeq$3% there is no X/Cu site interchange; furthermore, the observed values of the static disorder σ^2_{stat} are typical of values seen in well-ordered compounds. Basically, the XAFS results are consistent with a very high degree of order for the flux-grown crystals. We thus believe that Kondo disorder is not a significant factor for these compounds. (A possible exception is YbZnCu$_4$ for which we could not analyze the Zn K-edge XAFS because it is superimposed on the Cu K-edge XAFS. Given the chemical similarity of Zn and Cu, Zn/Cu site disorder seems a real possibility.)

A third problem for this analysis concerns the interpretation of the Yb L_3 x-ray absorption used to determine the occupation number $n_f(T)$. The analysis[9,14] relies on rather simple assumptions: the divalent and trivalent absorption edges are assumed to have the same shape and the same absorption matrix element, so that n_f is determined from the fractional weights of the two features. Similar assumptions are made for other methods (x-ray photoemission spectroscopy core levels; valence-band ultraviolet photoemission spectroscopy (UPS); Mossbauer isomer shift) for determining valence. While the resulting systematic error is not well understood, it has been argued[32] that the L_3 method is superior to use of isomer shift or lattice constant anomalies for the determination of valence. It has been pointed out[12] that the values of n_f estimated from the L_3 experiments are consistently and significantly larger than those estimated from valence-band photoemission. The latter estimate also requires the assumption of equal absorption matirix elements for the divalent and trivalent configurations and is extremely sensitive to choice of background. A point in favor of the use of x-ray absorption is that, unlike photoemission it truly samples the bulk of the compound; indeed it has been argued[13] that near-surface reconstruction gives rise to differences between the L_3 and UPS estimates of n_f. Whether this is so and what the systematic errors are in both measurements are, in our opinion, topics for future research. In any case, the deviations from the AIM that we observe for $n_f(T)$ using the L_3 measurement (Fig. 1) are qualitatively very similar to those observed for the effective moment (Fig. 2), the measurement of which is not subject to significant systematic error. (In our earlier paper[14] we showed that at room temperature for all cases except X=Ag, n_f is nearly equal to the effective moment.) The photoemission analysis yields an extremely slow crossover, to the extent that the hole occupancy is found to be $n_f \simeq 0.6$ in the high-temperature state of YbInCu$_4$ which is much smaller than the value (>0.9) that we have observed[33] using L_3. The latter value is, in our opinion, more realistic given the essentially trivalent behavior of the susceptibility of YbInCu$_4$ at high temperature.

We therefore argue that we have ruled out most of the major sources of error in our analysis, so that we can have a reasonable degree of confidence that the slow crossover is a real effect. As mentioned in the introduction, recent theory[10] for the ($S=1/2$) Anderson lattice, treated in the $1/d$ approximation (where d is the spatial dimension of the system) predicts such a slow crossover, referring to it as ''protracted screening.'' The degree of slowness is sensitive to the filling of the background conduction band; the crossover is slowest for partial filling of the background band. At present it is unclear the extent to which the effect depends on the orbital degeneracy.

The deviations of the data (Figs. 1 and 2) for YbXCu$_4$ from the predictions of the AIM are strongest for X=Mg, Zn, and Cd, weaker for X=Ag and weakest for X=Tl. We note that there is no correlation between this trend and the magnitude of the Kondo temperature (Table I) nor of the ground-state occupation number (Fig. 1). There *does* appear to be a correlation with the magnitude of the Hall coefficient for LuXCu$_4$: $R_0 = -1.8, -1.0$, and -0.8×10^{-10} m^3/C for X=Mg, Zn, Cd;[14] -0.6×10^{-10} m^3/C for X=Ag;[33] and $<1\times10^{-11}$ m^3/C for X=Tl.[14] This quantity can be taken as a measure of the conduction electron density in the background band. In a one-band model, where $R_0 = 1/ne$ and where there are 24 atoms in a unit cell of side 7.1 Å these values of R_0 correspond to the values 0.52, 0.93, 1.16, and 1.55 electrons per atom for the sequence {X=Mg, Zn, Cd, Ag}. While the one-band assumption is unrealistic, nevertheless these results suggest that the deviations from the AIM become weaker as the carrier density becomes larger. This accords with theory[10] which predicts no deviation for half filling of the background band and increasing deviation as the conduction-electron density decreases.

We should point out that a slow crossover is expected on rather general grounds. In the single impurity calculations the position of the chemical potential μ is set by the host metal conduction-band density of states, and the chemical potential is independent of temperature to order kT/W. In the hypothetical case of a periodic array of impurities that are noninteracting and incoherent the appreciable f weight and its asymmetric temperature dependence will lead to a significant temperature dependence of $\mu(T)$ and hence lead to a deviation of $n_f(T)$ from the behavior found in the solution to the single impurity model. It is not clear to us the extent to which this effect contributes to the predicted protracted screening.

In addition to our main conclusion, we would like to point to two more features of the analysis. The first is that the experimentally determined linear coefficients γ of specific

heat for $X=$Mg, Cd, Ag, and Zn are 20–30% larger than the values predicted by the AIM. This means that the experimental value of the Wilson ratio $\mathcal{R}$ is smaller than predicted by the AIM. This has been noticed before.[8,14] For $YbInCu_4$ there is excellent agreement between the experimental and calculated values; for $YbTlCu_4$ the calculated value of γ is 30% *smaller* than the experimental value. The second feature is that there is considerable disagreement between the measured and predicted values of the neutron line-shape parameters E_0 and Γ given in Table I. We remind the reader that the degree of systematic error for this determination is poorly understood, due to the difficulty of determining the nonmagnetic scattering for large T_K compounds. In addition, all Q dependence of the line shape in polycrystals is automatically averaged out. In the case of $YbInCu_4$, we have confidence in the results, since an alternate means of subtracting the nonmagnetic scattering[15] agrees with the method used here and since a neutron-scattering study of a single crystal[7] showed that the Q dependence of the line shape is quite small. For that case we note that the experimental peak energy E_0 agrees well with the prediction of the AIM but the measured linewidth Γ is a factor of 2 smaller than predicted, as though the spin fluctations have a longer lifetime than predicted by the AIM. On the other hand for $YbMgCu_4$, $YbTlCu_4$, and $YbZnCu_4$ the experimental values of peak energy differ significantly from the calculated values and the linewidths are *larger* than the predicted values. Such a large linewidth could be a consequence of a Q dependence of the peak parameter $E_0(Q)$; studies of single crystals are necessary to establish whether such a Q dependence is present. Finally we note that if the line-shape parameters for $YbAgCu_4$ are increased by 10% to account for the 10% smaller value of T_{max} observed for the neutron sample, they are in excellent agreement with the AIM predictions.

In conclusion, we have given evidence that the crossover from low-temperature Fermi-liquid behavior to high-temperature local-moment behavior is slower for periodic intermediate valence compounds than predicted by the Anderson impurity model. We have included supporting experiments to rule out the possibility that the disagreements between the data and the AIM predictions are due to large crystal fields or to Kondo disorder. We feel that the results are fairly robust. It will be interesting to see whether similar protracted screening is observed in other compounds, especially in those based on Ce where the orbital degeneracy is smaller ($N_J=6$) and where the size of the $4f$ orbital is considerably larger.

ACKNOWLEDGMENTS

Work at UC Irvine was supported by UCDRD funds provided by the University of California for the conduct of discretionary research by the Los Alamos National Laboratory. Work at Polytechnic was supported by Grant No. DOE FG02ER84-45127. Work at Lawrence Berkeley National Laboratory was supported by the Office of Basic Energy Sciences (OBES), Chemical Sciences Division of the Department of Energy (DOE), Contract No. DE-AC03-76SF00098. Work at Los Alamos was performed under the auspices of the DOE. Work at Argonne was supported by the DOE Office of Science under Contract No. W-31-109-ENG-38. The XAFS experiments were performed at SSRL, which is operated by the DOE/OBES.

[1] A. C. Hewson, *The Kondo Problem to Heavy Fermions* (Cambridge University Press, Cambridge, England, 1993), p. 315.

[2] N. Grewe and F. Steglich, in *Handbook on the Physics and Chemistry of Rare Earths*, edited by K. A. Gschneidner, Jr. and L. Eyring (Elsevier, Amsterdam, 1991), Vol. 14, p. 343.

[3] Various papers in *Proceedings of the International Conference on Strongly Correlated Electron Systems* [Physica B **259-261**, 353–432 (1999)].

[4] A. J. Millis and P. A. Lee, Phys. Rev. B **35**, 3394 (1987).

[5] A. Hasegawa and H. Yamagami, Prog. Theor. Phys. Suppl. **108**, 27 (1992).

[6] W. P. Beyermann, G. Grüner, Y. Dalicheouch, and M. B. Maple, Phys. Rev. Lett. **60**, 216 (1988).

[7] J. M. Lawrence, S. M. Shapiro, J. L. Sarrao, and Z. Fisk, Phys. Rev. B **55**, 14 467 (1997).

[8] T. Graf, J. M. Lawrence, M. F. Hundley, J. D. Thompson, A. Lacerda, E. Haanappel, M. S. Torikachvili, Z. Fisk, and P. C. Canfield, Phys. Rev. B **51**, 15 053 (1995).

[9] J. M. Lawrence, G. H. Kwei, P. C. Canfield, J. G. DeWitt, and A. C. Lawson, Phys. Rev. B **49**, 1627 (1994).

[10] A. N. Tahvildar-Zadeh, M. Jarrell, and J. K. Freericks, Phys. Rev. B **55**, R3332 (1997).

[11] A. N. Tahvildar-Zadeh, M. Jarrell, and J. K. Freericks, Phys. Rev. Lett. **80**, 5168 (1998).

[12] J. J. Joyce, A. J. Arko, J. L. Sarrao, K. S. Graham, Z. Fisk, and P. S. Riseborough, Philos. Mag. B **99**, 1 (1999).

[13] F. Reinert, R. Claessen, G. Nicolay, D. Ehm, S. Hüfner, W. P. Ellis, G.-H. Kweon, J. W. Allen, B. Kindler, and W. Assmus, Phys. Rev. B **58**, 12 808 (1998).

[14] J. L. Sarrao, C. D. Immer, Z. Fisk, C. H. Booth, E. Figueroa, J. M. Lawrence, R. Modler, A. L. Cornelius, M. F. Hundley, G. H. Kwei, R. Movshovich, J. D. Thompson, and F. Bridges, Phys. Rev. B **59**, 6855 (1999).

[15] J. M. Lawrence, R. Osborn, J. L. Sarrao, and Z. Fisk, Phys. Rev. B **59**, 1134 (1999).

[16] N. E. Bickers, D. L. Cox, and J. W. Wilkins, Phys. Rev. B **36**, 2036 (1987).

[17] Y. Kuramoto and E. Müller-Hartmann, J. Magn. Magn. Mater. **52**, 122 (1985).

[18] Y. Kuramoto, Z. Phys. B: Condens. Matter **53**, 37 (1983).

[19] E. Figueroa, J. M. Lawrence, J. L. Sarrao, Z. Fisk, M. F. Hundley, and J. D. Thompson, Solid State Commun. **106**, 347 (1998).

[20] P. Monachesi and A. Continenza, Phys. Rev. B **54**, 13 558 (1996).

[21] E. A. Goremychkin and R. Osborn, Phys. Rev. B **47**, 14 280 (1993).

[22] A. Severing, A. P. Murani, J. D. Thompson, Z. Fisk, and C.-K. Loong, Phys. Rev. B **41**, 1739 (1990).
[23] J. He, N. Tsujii, K. Yoshimura, K. Kosuge, and T. Goto, J. Phys. Soc. Jpn. **66**, 2481 (1997).
[24] C. H. Booth, D. E. MacLaughlin, R. H. Heffner, R. Chau, M. B. Maple, and G. H. Kwei, Phys. Rev. Lett. **81**, 3960 (1998).
[25] J. M. Lawrence, G. H. Kwei, J. L. Sarrao, Z. Fisk, D. Mandrus, and J. D. Thompson, Phys. Rev. B **54**, 6011 (1996).
[26] E. D. Crozier, J. J. Rehr, and R. Ingalls, in *X-Ray Absorption: Principles, Applications, Techniques of EXAFS, SEXAFS, XANES*, edited by D. Konigsberger and R. Prins (Wiley, New York, 1988), p. 373.
[27] G. G. Li, F. Bridges, and C. H. Booth, Phys. Rev. B **52**, 6332 (1995).
[28] C. H. Booth, F. Bridges, G. H. Kwei, J. M. Lawrence, A. L. Cornelius, and J. J. Neumeier, Phys. Rev. Lett. **80**, 853 (1998).
[29] E. A. Stern, Phys. Rev. B **48**, 9825 (1993).
[30] A. Severing, E. Gratz, B. D. Rainford, and K. Yoshimura, Physica B **163**, 409 (1990).
[31] O. O. Bernal, D. E. MacLaughlin, H. G. Lukefahr, and B. Andraka, Phys. Rev. Lett. **75**, 2023 (1995).
[32] J. Röhler, J. Magn. Magn. Mater. **47&48**, 175 (1985).
[33] A. L. Cornelius, J. M. Lawrence, J. L. Sarrao, Z. Fisk, M. F. Hundley, G. H. Kwei, J. D. Thompson, C. H. Booth, and F. Bridges, Phys. Rev. B **56**, 7993 (1997).